Revista Virtual de Química

ISSN 1984-6835

Artigo

Theoretical and Experimental Studies of the Interaction between Human Serum Albumin and Artepillin C, an Active Principle of the Brazilian Green Propolis

Chaves, O. A.; Pires, L. O.; Castro, R. N.; Sant'Anna, C. M. R.;* Netto-Ferreira, J. C.

Rev. Virtual Quim., **2019**, *11* (5), 1562-1578. Data de publicação na Web: 28 de outubro de 2019

http://rvq.sbq.org.br

Estudo Teórico e Experimental da Interação entre Albumina Sérica Humana e Artepillin C, um Princípio Ativo da Própolis Verde Brasileira

Resumo: A própolis verde brasileira é produzida na região sudeste do país pelas abelhas *Apis mellifera*, que utilizam como fonte de extração as plantas da espécie *Baccharis dracunculifolia*. Esse tipo de própolis apresenta diversas atividades biológicas, as quais estão geralmente atreladas à presença do composto natural Artepillin C. Albumina sérica humana (ASH) é o principal carreador de pequenas moléculas na corrente sanguínea e, tendo em vista o potencial farmacológico da Artepillin C, o objetivo do presente trabalho é o estudo da interação ASH:Artepillin C por técnicas espectroscópicas (dicroísmo circular, fluorescência no estado estacionário e resolvida no tempo), potencial zeta e ancoramento molecular. A interação ASH:Artepillin C ocorre no estado fundamental no sítio I da albumina, sendo controlada tanto pela entropia quanto pela entalpia. A presença de Artepillin C acarreta uma pequena perturbação na estrutura secundária da albumina e nenhum tipo de perturbação significativa em sua superfície. Estudos de ancoramento molecular sugerem que as principais forças controladoras da interaçãoASH:Artepillin C são van der Waals, hidrofóbica e ligação de hidrogênio.

Palavras-chave: Própolis verde brasileira; Artepillin C; albumina sérica humana; espectroscopia; ancoramento molecular.

Abstract

The Brazilian green propolis is produced in the south eastern region of the country by *Apis mellifera* bees, which use plants of the species *Baccharis dracunculifolia* as a source of extraction. This type of propolis has several biological activities, which are usually linked to the presence of the natural compound Artepillin C. Human serum albumin (HSA) is the main carrier of small molecules in the bloodstream and, in view of the pharmacological potential of Artepillin C, the main goal of the present work is the study of the interaction HSA:Artepillin C by spectroscopic techniques (circular dichroism, steady-state and time-resolved fluorescence), zeta potential and molecular docking. The interaction HSA:Artepillin C occurs in the ground-state at the site I of albumin and is entropically and enthalpically driven. The presence of Artepillin C entails a small perturbation on the secondary structure of the albumin and no significant perturbation on its surface. Molecular docking studies suggest that the main controlling forces of the interaction HSA:Artepillin C are van der Waals, hydrophobic and hydrogen bonding.

Keywords: Brazilian green propolis; Artepillin C, human serum albumin; spectroscopy; molecular docking.

* Instituto de Química, Departamento de Química Fundamental, Universidade Federal Rural do Rio de Janeiro, CEP 23890-000, Seropédica-RJ, Brazil.

santanna@ufrrj.br

DOI: 10.21577/1984-6835.20190109

Volume 11, Número 5 Setembro-Outubro 2019

Revista Virtual de Química
ISSN 1984-6835

Theoretical and Experimental Studies of the Interaction between Human Serum Albumin and Artepillin C, an Active Principle of the Brazilian Green Propolis

Otávio Augusto Chaves,[a,b] Lucas de Oliveira Pires,[b] Rosane Nora Castro,[b] Carlos Maurício R. Sant'Anna,[c,*] José Carlos Netto-Ferreira[b,d]

[a] Instituto SENAI de Inovação em Química Verde, Rua Morais e Silva 53, Maracanã, CEP 20271-030, Rio de Janeiro-RJ, Brasil.

[b] Universidade Federal Rural do Rio de Janeiro, Instituto de Química, Departamento de Química Orgânica, CEP 23890-000, Seropédica-RJ, Brasil.

[c] Universidade Federal Rural do Rio de Janeiro, Instituto de Química, Departamento de Química Fundamental, CEP 23890-000, Seropédica-RJ, Brasil.

[d] Instituto Nacional de Metrologia, Qualidade e Tecnologia-INMETRO, Divisão de Metrologia Química, CEP 25250-020, Duque de Caxias-RJ, Brasil.

* santanna@ufrrj.br

Recebido em 30 de setembro de 2019. Aceito para publicação em 30 de setembro de 2019

1. Introduction

Propolis is a complex mixture prepared by bees inside their hives as a protective barrier used for thermal insulation and microbiological control.[1] This product shows

peculiar physicochemical characteristics and biological properties, essential to bee life. It is produced in the hive from resinous, sticky and balsamic substances collected by the bees from various materials (leaves, buds, floral buds, and plant secretions) from different species of plants. After these components have been harvested in the field, they are assembled within the colony, where they are supplemented by varying amounts of wax, pollen, salivary secretions and enzymes.[2] Since propolis plays an important role in the prevention of diseases related to the bee health, this knowledge has leveraged the application of this natural product to human therapies for centuries.[3] The biological properties of propolis are often related to the presence of polyphenolic substances, mainly of the class of phenylpropanoids and several classes of flavonoids, with the quantification and identification of such substances being considered standards for assessing the quality of propolis worldwide.[4,5]

The Brazilian green propolis is produced mainly by Africanized honey bees (*Apis mellifera*) in the south eastern region of Brazil, having as main plant source the species *Baccharis dracunculifolia* (also known as *alecrim-do-campo*).[6] Its high commercial and scientific value is related to its biological properties, such as antimicrobial, antitumor, anti-inflammatory and antioxidant. These biological activities are often related to the presence of the chemical marker called (*E*)-3-[4-hydroxy-3,5-bis(3-methylbut-2-enyl)phenyl]prop-2-enoic acid (Artepillin C – Figure 1).[7,8]

Human serum albumin (HSA) has a molecular weight of 66,437 Da (based on amino acid composition) and is the most abundant protein in human plasma (concentration around 600 µM). Commercial preparations contain varying degrees of post-translational modifications and genetic variants with molecular weight components mainly in the range of 66,437 to 66,600 Da.[9] HSA displays an extraordinary binding capacity to the ligand, providing a depot and carrier for many endogenous and exogenous compounds. In fact, HSA represents the main carrier for fatty acids, affects the pharmacokinetics of many drugs, provides the metabolic modification of some ligands, renders potential toxins harmless, accounts for most of the anti-oxidant capacity of human plasma, and exhibits (pseudo-) enzymatic properties.[10,11] Mainly because of the biological importance of HSA in the biodistribution of exogenous molecules in the human bloodstream, there are several studies in the literature involving HSA and natural products, *e.g.* hesperetin,[12] alpinetin,[13] naringin,[14] glucopyranosyl-dihydroxyflavonol,[15] plumeran indole alkaloid,[16] genistein, and curcumin.[17]

Considering that Artepillin C has important biological properties and is an abundant constituent of Brazilian green propolis, whereas HSA is an important protein to the biodistribution of exogenous molecules in human plasma, the present study reports the interaction between HSA and Artepillin C through spectroscopic techniques (circular dichroism, steady-state and time-resolved fluorescence) combined with zeta potential and molecular docking calculation.

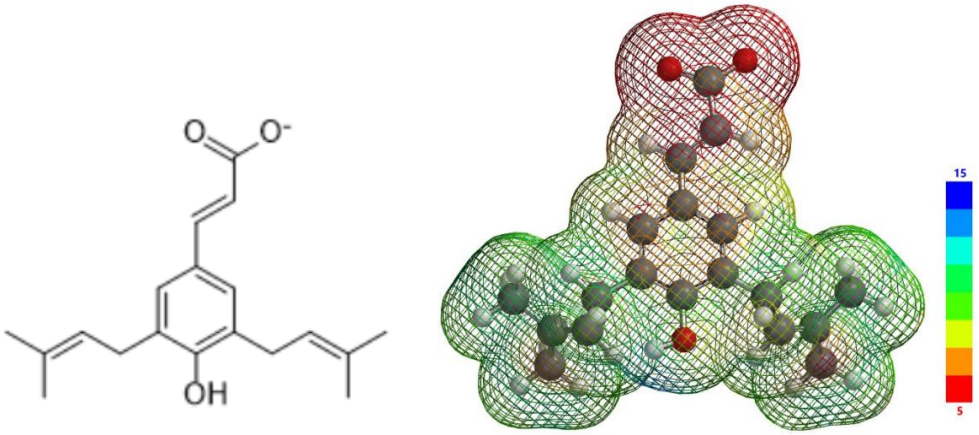

Figure 1. Chemical structure of Artepillin C and its corresponding theoretical local ionization potential map at pH = 7.4

2. Experimental

2.1. Materials and instruments

Commercially available HSA, PBS buffer (pH = 7.4), warfarin, ibuprofen and digitoxin were obtained from Sigma-Aldrich Chemical Company. Water used in all experiments was Millipore grade. Methanol (spectroscopic grade), hexane, dichloromethane, chloroform, glacial acetic acid and acetone were obtained from Tedia Ltd.

The main Artepillin C fraction was purified by semi-preparative high efficiency liquid chromatography employing a C-18 column (250 × 10 mm × 5 µm) from Shimadzu. The melting point for Artepillin C was determined on a Meltemp II apparatus. Nuclear magnetic resonance (^{1}H and ^{13}C) spectra were recorded on a Bruker Avance III spectrometer (500 MHz) using tetramethylsilane (TMS) as internal standard and deuterated methanol as solvent.

For the studies of the interaction between HSA and Artepillin C, UV-Vis and steady-state fluorescence spectra were measured on a Jasco J-815 fluorimeter using a quartz cell (1.00 cm optical path), employing a thermostatic cuvette holder Jasco PFD-425S15F. Time-resolved fluorescence measurements were performed on a spectrofluorimeter model FL920 CD, from Edinburgh Instruments, equipped with an EPL laser (λ_{exc} = 280 ± 10 nm; pulse of 850 ps with energy of 1.8 µW/pulse, monitoring emission at 340 nm). Circular dichroism (CD) spectra were obtained using a Jasco J-815 spectropolarimeter equipped with a Jasco PFD-425S15F thermostated system with 0.1 °C accuracy. Zeta potential (ZP) for HSA and HSA:Artepillin C were measured in a NanoBrook ZetaPALS. All measurements were performed with 10 runs at room temperature (*ca* 298 K) and the results were reported in terms of ZP ± SD, where SD is the standard deviation.

2.2. Preparation of n-hexane extract from Brazilian green propolis

Artepillin C was isolated from a sample of crude green propolis obtained directly from producers in the city of Carmo (Rio de Janeiro - Brazil) in the year of 2012. For the isolation of the biomarker, 3.00 g of pulverized green propolis were extracted with 150 mL of *n*-hexane using Soxhlet apparatus for 6 hours. After the extraction, the solvent was removed under reduced pressure. The obtained crude extract was solubilized in 3.0 mL of dichloromethane and to remove the wax and

resin content, this solution was diluted with 20 mL of methanol, left overnight in the freezer and then vacuum filtered and concentrated on an evaporator (300 mg).

2.3. Artepillin C isolation from the n-hexane extract

The *n*-hexane extract of the Brazilian green propolis (300 mg) was initially purified by open-column liquid chromatography, using as a stationary phase silica gel previously activated in an oven at 100 °C for 1 hour. The mobile phase consisted of mixtures of chloroform and acetone in increasing polarity gradient (0-20 % acetone). Thin layer chromatography was used to monitor the column chromatography, using acetone:*n*-hexane (40:60, v/v) containing few drops of glacial acetic acid as the mobile phase. Thus, the fractions exhibiting chromatic similarity were pooled and concentrated under reduced pressure. The main fraction obtained after the open column chromatography (90 mg) was purified by semipreparative high efficiency liquid chromatography employing a C-18 column. The mobile phase consisted of mixtures of acetonitrile and MilliQ water, with increasing gradient elution (72-100 %, in 18 minutes), and the peaks obtained were monitored employing an UV detector at 280 nm. The substance eluted in 6.0 minutes (Artepillin C) was concentrated in an evaporator, yielding 24 mg of a white solid (98 % chromatographic purity - HPLC-DAD). It was characterized as the natural product Artepillin C by melting point (97-99 °C), ^{1}H and ^{13}C NMR (Table 1), being in full agreement with the literature.[18]

Table 1. ^{1}H and ^{13}C NMR data for Artepillin C

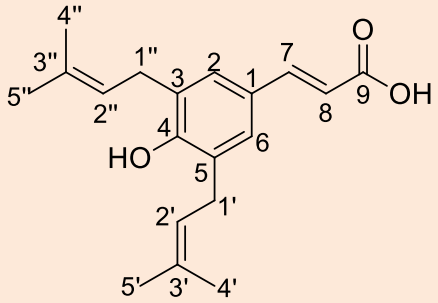

C	δ H (ppm)	δ C (ppm)
1	-	126.27
2/6	7.20 (2H, *s*)	128.30
3/5	-	127.58
4-OH	-	155.32
7	7.70 (1H, *d*, *J*=15,9 Hz)	147.29
8	6.29 (1H, *d*, *J*=15,9 Hz)	114.01
9-CO	-	177.65
1'/1''	3.35 (4H, *d*, *J*=7,1 Hz)	29.36
2'/2''	5.31 (2H, *t*, *J*=7,1 Hz)	121.19
3'/3''	-	135.04
4'/4''	1.79 (*s*, 6H)	25.79
5'/5''	1.78 (*s*, 6H)	17.93

2.4. Spectroscopic measurements for HSA binding studies

All spectra were recorded with appropriate background corrections. Inner filter correction was done for all steady-state fluorescence data, since the UV absorption for the ligand is greater than 0.10 a.u. at 280 and 340 nm (4.65 × 10^{-6} M, in PBS).[19]

$$F_{cor} = F_{obs} 10^{[(A_{ex}+A_{em})/2]} \quad (1)$$

where F_{cor} and F_{obs} are the corrected and observed steady-state fluorescence intensity values, while A_{ex} and A_{em} represent absorbance values at the excitation (λ = 280 nm: ε = 209,697 $cm^{-1}M^{-1}$, in PBS) and emission wavelengths (λ = 340 nm: ε = 35,153 $cm^{-1}M^{-1}$, in PBS).

The UV-Vis absorption spectrum for Artepillin C (4.65 × 10^{-6} M, in PBS) was measured in the 200-500 nm range at 310 K. The steady-state fluorescence measurements were carried out for 3.0 mL of HSA solution (1.00 × 10^{-5} M, in PBS) without and in the presence of Artepillin C in the 290-450 nm range (λ_{exc} = 280 nm) at 289 K, 296 K, 303 K, 310 K and 317 K. The addition of Artepillin C to the HSA solution was done manually by using a microsyringe, achieving final concentrations of 0.67; 1.33; 2.00; 2.66; 3.32; 3.65; 3.98, and 4.65 × 10^{-6} M.

The quenching of HSA fluorescence in the presence of increasing concentrations of Artepillin C was analyzed using the Stern–Volmer equation (equation 2A) and the k_q definition (equation 2B):[20]

$$\text{(A)} \quad \frac{F_0}{F} = 1 + k_q \tau_0 [Q] = 1 + K_{SV}[Q] \quad \text{(B)} \quad k_q = \frac{K_{SV}}{\tau_0} \quad (2)$$

where F_0 and F represent the fluorescence intensity values of the HSA in the absence and presence of the Artepillin C, respectively, [Q] is the ligand concentration. K_{SV} and k_q are the Stern-Volmer constant and the bimolecular quenching rate constant, respectively. τ_0 is the lifetime of the fluorophore in the absence of ligand - the measured average value for the fluorescence lifetime of HSA was (5.72 ± 0.11) × 10^{-9} s.

Data from the fluorescence quenching experiments were used to calculate the modified Stern-Volmer binding constant (K_a) of HSA with Artepillin C according to the modified Stern–Volmer equation – equation 3:[21]

$$\frac{F_0}{F_0 - F} = \frac{1}{f[Q]K_a} + \frac{1}{f} \quad (3)$$

where F_0 and F are the steady-state fluorescence intensities in the absence and presence of Artepillin C, respectively; f is the fraction of the initial fluorescence intensity corresponding to fluorophore that is accessible to the quencher ($f \approx 1.00$) and [Q] is the Artepillin C concentration.

The thermodynamic parameters $\Delta H°$ and $\Delta S°$, the enthalpy and entropy change, respectively, for the HSA:Artepillin C

interaction were obtained from van't Hoff plot using equation 4A. Gibb's free energy change values ($\Delta G°$) were obtained from equation 4B:[22]

$$(A)\quad \ln K_a = -\frac{\Delta H^0}{RT} + \frac{\Delta S^0}{R} \qquad (B)\quad \Delta G^0 = \Delta H^0 - T\Delta S^0 \qquad (4)$$

where T is the temperature (289 K, 296 K, 303 K, 310 K and 317 K), R is the gas constant (8.3145 $Jmol^{-1}K^{-1}$) and K_a is the effective quenching constant for the accessible fluorophores, which is analogous to associative binding constant (modified Stern-Volmer binding constant) for the quencher (Artepillin C) and acceptor (HSA) system.

Time-resolved fluorescence decays for the free HSA solution (1.00×10^{-5} M in PBS) and for a HSA solution containing the maximum concentration of Artepillin C used in the steady-state fluorescence studies (4.65×10^{-5} M, in PBS) was obtained at room temperature (*ca* 298 K).

For the CD measurements, HSA concentration was kept constant at 1.00×10^{-6} M and the Artepillin C concentration was set as the maximum concentration used in the steady-state fluorescence studies (4.65×10^{-6} M). CD spectra were measured in the 200-250 nm range, at 310 K. All spectra were recorded with appropriate background corrections.

The intensity of the CD signal was expressed as mean residue ellipticity (MRE), defined according to equation 5:

$$MRE = \frac{\theta}{(10.n.l.C_P)} \qquad (5)$$

where ϑ is the observed CD (in millidegrees), n is the number of amino acid residues (585 for HSA),[23] l is the path length of the cell (in cm) and C_p is the molar concentration of HSA (1.00×10^{-6} M). The α-helical contents of free HSA and bound to Artepillin C were calculated from the molar residual ellipticity (MRE) values at 208 nm (equation 6A) and 222 nm (equation 6B):[16,24]

$$\alpha\text{-}helix\% = \frac{(-MRE_{208} - 4000)}{(33000 - 4000)}\ x\ 100 \qquad (6A)$$

$$\alpha\text{-}helix\% = \frac{(-MRE_{222} - 2340)}{30300}\ x\ 100 \qquad (6B)$$

Competitive binding studies were carried out with the three probes widely employed for the characterization of binding sites in HSA, *i.e.*, warfarin, ibuprofen, and digitoxin for site I, II, and III, respectively. HSA and site probes were used at a fixed concentration (1.00×10^{-5} M – proportion 1:1) and the fluorescence quenching titration with Artepillin C was performed as described previously in the steady-state fluorescence quenching method, at 296 K.

2.5. Zeta potential measurements for the interaction HSA:Artepillin C

The surface charge of HSA in the absence and presence of Artepillin C was characterized in terms of zeta potential (ZP). The ZP was measured for HSA solution (1.00×10^{-5} M, in PBS solution) without and in the presence of the maximum ligand concentration used in the steady-state fluorescence experiments (4.65×10^{-6} M), at room temperature (*ca* 298 K).

2.6. Theoretical calculations

The Artepillin C structure was energy-minimized by Density Functional Theory (DFT) calculations, with B3LYP function and 6-31G* basis set,[25,26] available in Spartan' 14 program.[27] The crystallographic structure of HSA was obtained from Protein Data Bank (1N5U).[23] The molecular docking studies were performed with GOLD 5.5 program (CCDC, *Cambridge Crystallographic Data Centre*).[28]

The hydrogen atoms were added to the albumin structure according to the data inferred by GOLD 5.5 program on the ionization and tautomeric states. Docking interaction cavity in the protein was established with a 10 Å radius from the Trp-214 residue. The scoring function used was '*ChemPLP*', which is the default function of the GOLD 5.5 program.[28] The graphical representation of the best score was generated with PyMOL program (DeLano Scientific LLC).[29] For more details, see previous publications.[30,31]

3. Results and Discussion

3.1. Binding ability of Artepillin C toward HSA

There are numerous molecular interactions responsible for decreasing the fluorescence intensity in a protein after its interaction with small molecules, *e.g.* collisional deactivation, electronic energy transfer, excited state reactions, and complex formation. This phenomenon is called fluorescence quenching.[32] Usually the intrinsic fluorescence of a protein originates from the aromatic amino acids tryptophan (Trp), tyrosine (Tyr) and/or phenylalanine (Phe). However, the indole group of the Trp residue is the dominant source of UV absorbance and fluorescence emission in the protein. In the case of human serum albumin, for λ_{exc} = 280 nm the maximum emission of fluorescence at λ_{em} = 340 nm shows no contribution of either Phe or Tyr. Therefore, Trp residue is the major responsible for the fluorescence of HSA.[33,34] Figure 2A shows the effect of Artepillin C on the fluorescence intensity of HSA. Although Artepillin C exhibits weak fluorescence at the highest concentration tested (Figure 2A in horizontal dashed line), its maximum emission wavelength does not overlap with that of HSA, thus resulting in no effect on the fluorescence measurements. As shown in the Figure 2A, there is a weak red shift in the maximum steady-state fluorescence emission of albumin upon the maximum ligand addition (from 340 to 343 nm), suggesting that the amino acid residues around Trp-214 residue are in a more polar environment in the presence of Artepillin C.[35]

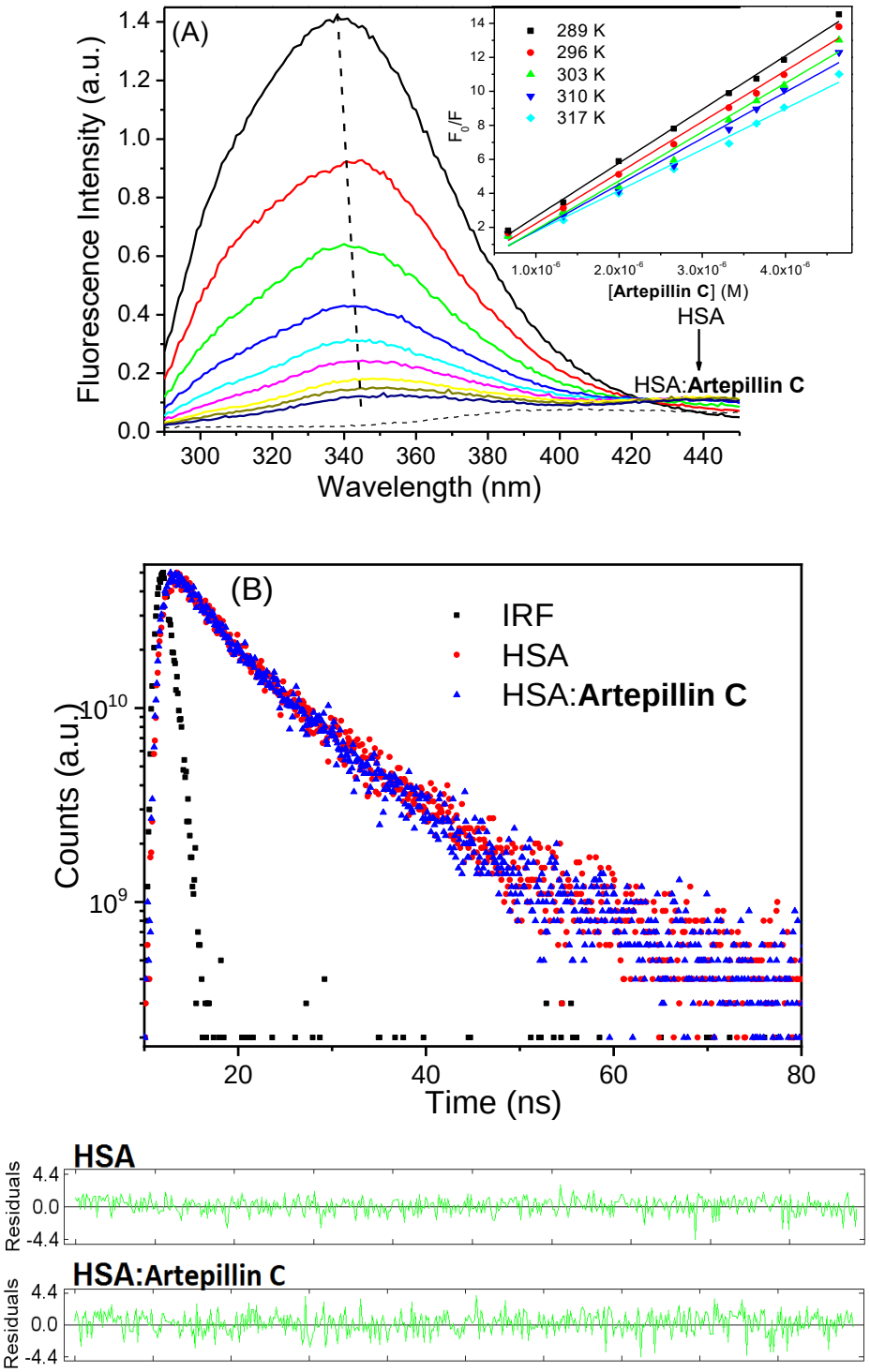

Figure 2. (A) Steady-state fluorescence emission of HSA and its quenching by successive additions of Artepillin C at pH = 7.4 and 310 K. *Inset*: Stern-Volmer plots at five different temperatures (289 K, 296 K, 303 K, 310 K and 317 K) for the interaction HSA:Artepillin C. (B) Time-resolved decays for HSA without and in the presence of the maximum ligand concentration used in the steady-state fluorescence measurements. [HSA] = 1.00×10^{-5} M and [Artepillin C] = 0.67; 1.33; 2.00; 2.66; 3.32; 3.65; 3.98, and 4.65×10^{-6} M

The fluorescence quenching mechanism of a protein, *i.e.* static or dynamic process, can be determined by calculating either the quenching rate constant of a system under different temperatures, or the fluorescence lifetime of a protein in the absence and presence of the ligand under study.[36] From the steady-state fluorescence data and by carrying out a Stern-Volmer analysis (*inset* in the Figure 2A), both Stern-Volmer constant (K_{SV}) and bimolecular quenching rate constant (k_q) can be calculated. To distinguish dynamic quenching from static quenching, one must investigate the changes in K_{SV} and k_q with temperature. As can be seen in Table 2, both K_{SV} and k_q values decrease with increasing temperature, resulting in decreased stability of HSA:Artepillin C complex formation at high temperature.[37] Since k_q values are larger than the diffusion rate constant in water ($k_{diff} \approx 7.40 \times 10^9$ $M^{-1}s^{-1}$, according to Smoluchowski-Stokes-Einstein theory at 298 K),[38] indicate that the fluorescence quenching takes place *via* a static process. This static mechanism probably originates from a ground-state association between Trp-214 and the natural product Artepillin C.[16]

To further confirm that static mechanism is the main fluorescence quenching process in the interaction HSA:Artepillin C, time-resolved fluorescence measurements were carried out for HSA without and in the presence of the natural product. Figure 2B depicts time-resolved fluorescence decays for HSA and HSA:Artepillin C. Free HSA showed two fluorescence lifetimes (τ_1 = 1.45 ± 0.14 ns, 12.0 % contribution and τ_2 = 5.72 ± 0.11 ns,, 88.0 % contribution – χ^2 = 1.098), which is in full agreement with literature results.[39] After the addition of Artepillin C to the HSA solution, the albumin fluorescence lifetime did not undergo any change within the experimental error (τ_1 = 1.41 ± 0.11 ns, 15.0 % contribution and τ_2 = 5.67 ± 0.10 ns,, 85.0 % contribution – χ^2 = 1.101). This result is consistent with a ground-state association between the albumin and Artepillin C, confirming the static quenching mechanism proposed by steady-state fluorescence measurements.[31,35]

Table 2. Binding constant values (K_{SV}, k_q and K_a) and thermodynamic parameters ($\Delta H°$, $\Delta S°$ and $\Delta G°$) for the interaction between HSA:Artepillin C at 289 K, 296 K, 303 K, 310 K and 317 K

T (K)	K_{SV} ($\times 10^4$) (M^{-1})	k_q($\times 10^{12}$) ($M^{-1}s^{-1}$)	K_a ($\times 10^5$) (M^{-1})	$\Delta H°$ (kJmol^{-1})	$\Delta S°$ (kJmol^{-1}K^{-1})	$\Delta G°$ (kJmol^{-1})
289	3.15±0.07	5.51	7.97±0.10			-32.6
296	2.99±0.10	5.23	6.58±0.07			-32.9
303	2.87±0.14	5.02	5.36±0.11	-19.9±1.10	0.0439±0.0015	-33.2
310	2.71±0.14	4.74	4.45±0.06			-33.5
317	2.41±0.10	4.21	3.88±0.07			-33.8

Obs: r^2 for K_{SV} and k_q: 0.9806-0.9966; r^2 for K_a: 0.9983-0.9999 and r^2 for $\Delta H°$, $\Delta S°$ and $\Delta G°$: 0.9989

Knowing the value for the modified Stern-Volmer binding constant (K_a) (eq. 3) between serum albumin and a ligand is important to understand its distribution in the plasma, body tissues and organs.[40] The K_a values are in the order of 10^5 M^{-1} (Table 2 and Figure 3A), indicating a moderate affinity between HSA and Artepillin C. These values are comparable to those observed for different natural products as reported in the literature.[12,15,17] Table 2 also shows that K_a values are inversely correlated with temperature. Furthermore, K_a perfectly matches the K_{sv} values obtained as described above (the same trend), which is

further evidence of a ground-state association between HSA and Artepillin C.[41]

When a ligand binds to a protein, there is the possibility of four types of non-covalent interactions, *i.e.*, hydrogen bonds, van der Waals forces, lipophilic and electrostatic interactions. The thermodynamic parameters ($\Delta H°$ and $\Delta S°$) are generally employed as evidence to identify the nature of the forces acting on a particular type of interaction, and were thus calculated for the pair HSA:Artepillin C according to the van't Hoff and Gibbs free energy analysis (Table 2 and Figure 3B).[34]

The negative values for $\Delta G°$ are consistent with the spontaneity of the interaction between HSA and Artepillin C. Since, both the negative value for $\Delta H°$ and the positive value for $\Delta S°$ can contribute positively to the negative sign of $\Delta G°$, the interaction of Artepillin C with albumin must be enthalpically and entropically driven.[42] From the point of view of water structure, a positive entropy has been considered as a typical signature of a hydrophobic effect, since the water molecules that are arranged in an orderly fashion around the ligand and the protein molecule acquire a more random configuration as a result of the hydrophobic effect.[40]

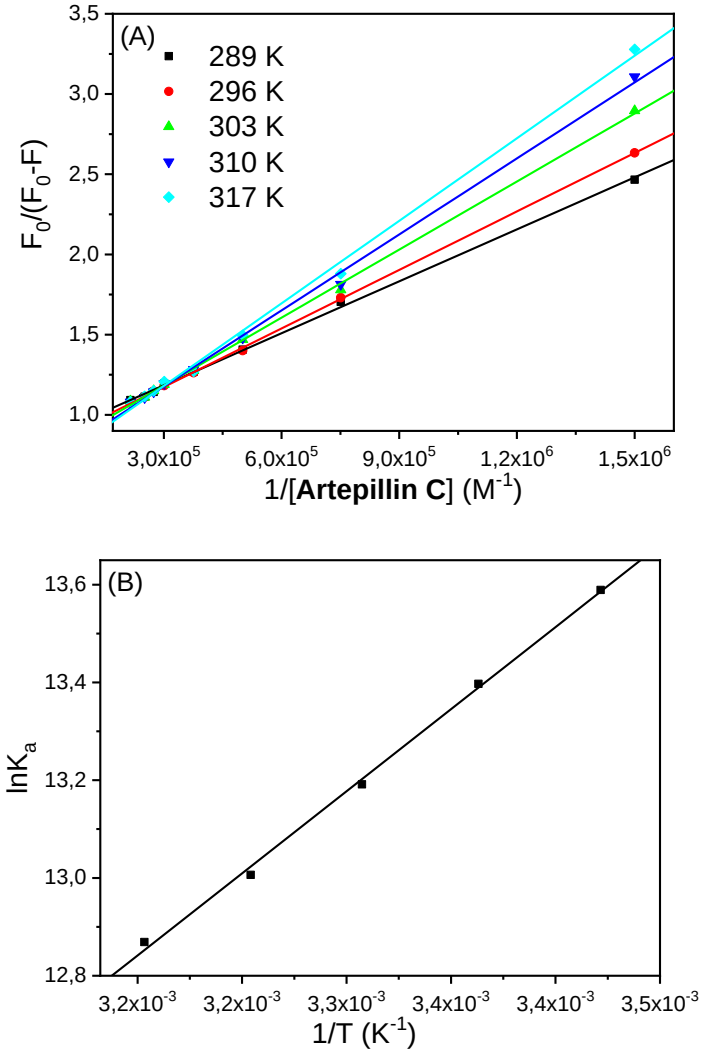

Figure 3. (A) Modified Stern-Volmer plots for the interaction HSA:Artepillin C at 289 K, 296 K, 303 K, 310 K and 317 K. (B) Van't Hoff plot for the interaction HSA:Artepillin C. [HSA] = 1.00 × 10^{-5} M and [Artepillin C] = 0.67; 1.33; 2.00; 2.66; 3.32; 3.65; 3.98 and 4.65 × 10^{-6} M

3.2. Perturbations on the HSA structure upon ligand binding

Circular dichroism (CD) is a sensitive technique to monitor conformational changes in a protein. The CD spectrum of HSA exhibits two negative signals at 208 and 222 nm, which correspond to π–π* and *n*–π* transitions, respectively.[43,44] Changes in these signals are widely used to investigate perturbations on the secondary structure of albumin upon ligand binding.[45] Figure 4 depicts the CD spectra for HSA in the absence and presence of the maximum ligand concentration used in the steady-state fluorescence measurement. It is worth noting that the CD signal decreased weakly its intensity upon ligand binding, suggesting that Artepillin C can only cause a weak perturbation on the secondary structure of the protein.[40] The α-helical % content for HSA at 208 and 222 nm were 63.9 % and 62.0 %, respectively. On the other hand, HSA:Artepilin C showed values of 62.5 % at 208 nm and 60.0 % at 222 nm. The weak decrease in the quantitative values for HSA after ligand binding can confirm the weak Artepillin C perturbation on the secondary albumin structure.[31]

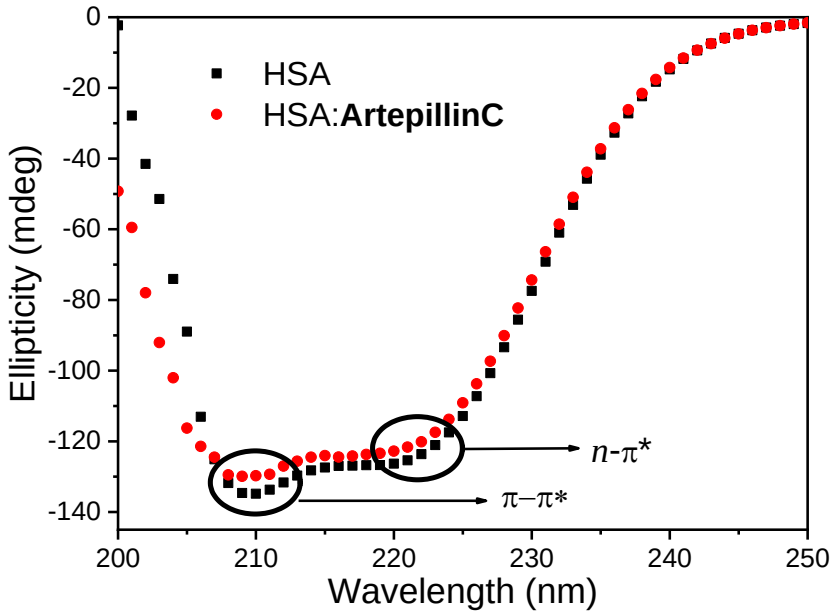

Figure 4. CD spectra for HSA without and in the presence of Artepillin C at pH = 7.4 and 310 K. [HSA] = 1.00 × 10^{-6} M and [Artepillin C] = 4.65 × 10^{-6} M

Variations in the zeta potential (ZP, ζ) for a protein can mainly imply in conformational changes and/or unfolding/denaturation processes in its protein structure.[46] Thus, the ZP of a protein can be used as an indicator of the protein stability upon ligand binding. Experimental ZP value for free HSA was negative (ζ ~ 7.19 ± 2.32 mV, conductance ~ 30,120 μS, and electric field ~ 13.10 V/cm) in PBS buffer solution. Moreover, with the addition of Artepillin C (4.65 × 10^{-6} M), ZP was ζ ~ 8.10 ± 1.46 mV, conductance ~ 28,943 μS, and electric field ~ 12.73 V/cm. It is important to note that the ZP value for HSA before and after addition of Artepillin C is the same inside the experimental error of the measurements, indicating that there is no significant structural change on the protein surface after ligand addition.[47]

3.3. Investigation of the main protein binding pocket and molecular docking analysis

The HSA structure shows two main binding pockets (namely site I and II) for different ligands. The protein pocket located in the subdomain IIA (site I) shows an affinity for a wide range of drugs, including warfarin, indomethacin, and phenylbutazone, while subdomain IIIA (site II) has affinity for ibuprofen, diazepam, and flufenamic acid. Recently, another main binding site has also been detected in the HSA structure (site III), which is located in the subdomain IB and has a high affinity for digitoxin.[48] In order to identify the main binding site of Artepillin C toward HSA structure, competitive binding measurements were carried out (Figure 5). The K_a values obtained in the presence of warfarin, ibuprofen, and digitoxin were (3.58 ± 0.10); (6.52 ± 0.12) and (5.85 ± 0.10) × 10^5 M, respectively, at 296 K. Comparing these results to the K_a value without the presence of each site marker at 296 K, it was concluded that there is a decrease of 45.6 %; 0.91 % and 11.1 % for the K_a value in the presence of warfarin, ibuprofen, and digitoxin, respectively, indicating that site I, where Trp-214 residue can be found, is the main binding site for Artepillin C.[31]

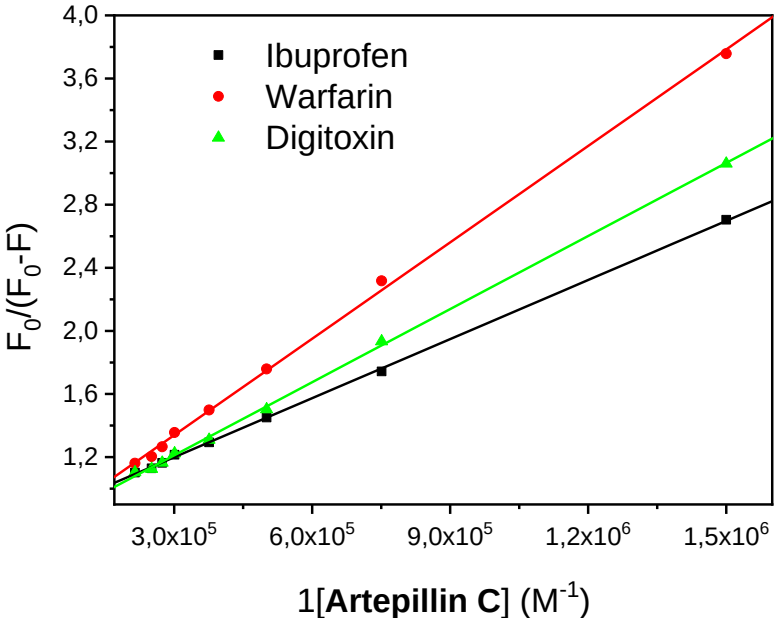

Figure 5. Modified Stern-Volmer plots for the interaction HSA:Artepillin C in the presence of three different site markers (warfarin, ibuprofen and digitoxin) at 296 K. [HSA] = 1.00 × 10^{-5} M and [Artepillin C] = 0.67; 1.33; 2.00; 2.66; 3.32; 3.65; 3.98, and 4.65 × 10^{-6} M

To provide an explanation at molecular level on the binding ability between HSA and Artepillin C, molecular docking calculations were performed, suggesting the main amino acid residues and major intermolecular forces involved in the HSA:Artepillin C interaction inside subdomain IIA (site I) - the main binding site detected by the competitive binding studies described above. Considering that the spectroscopic measurements were carried out at pH = 7.4 and knowing that the pK_a value of the carboxyl acid group present in the Artepillin C structure is 4.65,[49] molecular docking calculations were performed for the ionic form of the ligand. Figure 6 depicts the best docking pose for Artepillin C in the site I.

Molecular docking results suggested hydrogen bonding, van der Waals and hydrophobic interactions as the main binding forces. The hydrogen atom of the hydroxyl

group of the amino acid residues Ser-201 and Ser-453 is a potential donor for hydrogen bonding with carboxyl and phenol groups of the ligand structure, respectively, within a distance of 1.90 and 2.10 Å, respectively. The amino acid residue Trp-214 can interact *via* van der Waals forces with the ligand structure within a distance of 2.00 Å. On the other hand, Val-343 and Leu-480 residues can interact with the ligand structure *via* hydrophobic forces, within a distance of 2.70 and 2.80 Å, respectively.

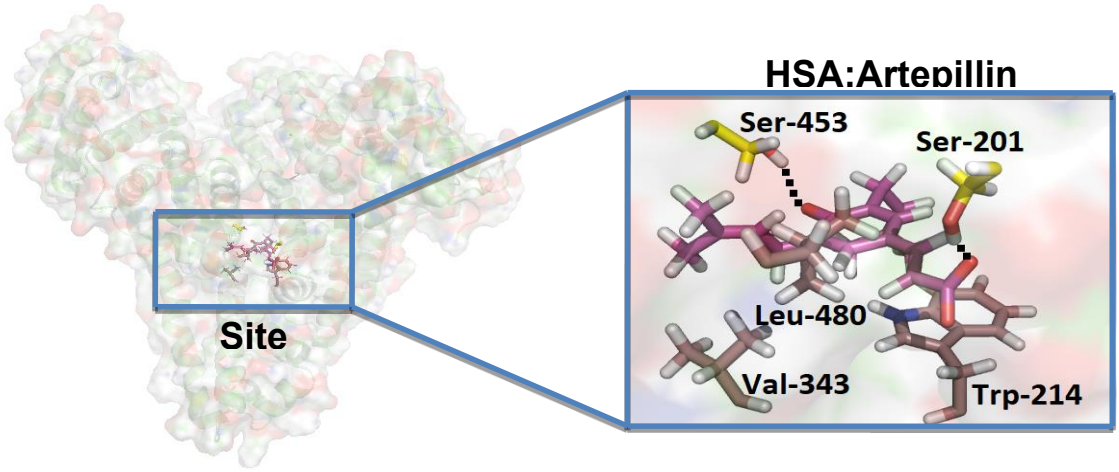

Figure 6. Best score pose for HSA:Artepillin C inside subdomain IIA (*ChemPLP* function). Artepillin C structure is represented in magenta, and the selected hydrophilic and hydrophobic amino acids residues are represented in yellow and brown, respectively. Black dots represent the interaction *via* hydrogen bonding. Hydrogen: white; oxygen: red and nitrogen: dark blue

4. Conclusion

Since K_{SV} values decreased with increasing temperature, suggest that the interaction between the natural product isolated from Brazilian green propolis (Artepillin C) and HSA occurs through a ground-state association (static quenching mechanism). This phenomenon is supported by k_q values which are higher than k_{diff} value, as well as fluorescence lifetime for HSA is practically the same without and in the presence of Artepillin C. The interaction HSA:Artepillin C is moderate and causes a very weak perturbation on the secondary structure of the albumin; however, there is no significant structural change on the surface of the protein. The interaction process is spontaneous and occurs mainly in the subdomain IIA (site I), where Trp-214 residue can be found. The interaction is enthalpically and entropically driven and molecular docking results suggested that Artepillin C can interact with the amino acid residues Trp-214; Ser-201; Val-343; Ser-453, and Leu-480 *via* hydrogen bonding, van der Waals and hydrophobic forces. This study can contribute to a better understanding of the pharmacokinetic profile of natural products, having a specific application on the medicinal ability of Artepillin C.

Acknowledgements

This study was financed in part by the Coordenação de Aperfeiçoamento de Pessoal de Nível Superior - Brasil (CAPES) - Finance Code 001.

This research was supported by the Brazilian funding agencies: Conselho Nacional de Desenvolvimento Científico e Tecnológico (CNPq) and Fundação de Amparo à Pesquisa do Estado do Rio de Janeiro (FAPERJ). The authors also acknowledge Prof. Dr. Nanci Camara de Lucas Garden (Institute of

Chemistry - UFRJ) for the time-resolved fluorescence facilities. O.A.C. acknowledges *Instituto Euvaldo Lodi* (IEL-Brazil) for the researcher grant at SENAI Innovation Institute for Green Chemistry (Encomenda Rhae Trainee II - 404988/2017-2 -Process: 350173/2018-4). J.C.N.-F. acknowledges INMETRO for a Visiting Professor fellowship.

References

[1] Funakoshi-Tago, M.; Okamoto, K.; Izumi, R.; Tago, K.; Yanagisawa, K.; Narukawa, Y.; Kiuchi, F.; Kasahara, T.; Tamura, H. Antiinflammatory activity of flavonoids in Nepalese propolis is attributed to inhibition of the IL-33 signaling pathway. *International Immunopharmacology* **2015**, *25*, 189. [CrossRef]

[2] Athikomkulchai, S.; Awale, S.; Ruangrungsi, N.; Ruchirawat, S.; Kadota, S. Chemical constituents of Thai propolis. *Fitoterapia* **2013**, *88*: 96. [CrossRef]

[3] Castaldo, S.; Capasso, F. Propolis, an old remedy in modern medicine. *Fitoterapia* **2002**, *73*, 1. [CrossRef]

[4] Huang, S.; Zhang, C. -P.; Wang, K.; Li, G. Q.; Hu, F. –L. Recent Advances in the Chemical Composition of Propolis. *Molecules* **2014**, *19*, 19610. [CrossRef]

[5] Lorenzon, M. C. A.; Castro, R. N.; Pires, L. O.; Koshiyama, A. S.; Bento, K. J. B. Biological values of different types of Brazilian propolis. *Greener Journal of Agricultural Sciences* **2018**, *8*, 90. [CrossRef]

[6] Alencar, S. M.; Aguiar, C. L.; Guzmán, J. P.; Park, Y. K. Composição química de Baccharis dracunculifolia, fonte botânica das própolis dos estados de São Paulo e Minas Gerais. *Ciência Rural* **2005**, *35*, 909. [CrossRef]

[7] Salgueiro, F. B.; Castro, R. N. Comparação entre a composição química e capacidade antioxidante de diferentes extratos de própolis verde. *Quimica Nova* **2016**, *10*, 1192. [CrossRef]

[8] Veiga, R. S.; de Mendonça, S.; Mendes, P. B.; Paulino, N.; Mimica, M. J.; Lagareiro Netto A. A.; Lira, I. S.; López, B. G.; Negrão, V.; Marcucci, M. C. Artepillin C and phenolic compounds responsible for antimicrobial and antioxidant activity of Green própolis and Baccharis dracunculifolia DC. *Journal of Applied Microbiology* **2017**, *122*, 911. [CrossRef]

[9] Trainor, G. L. The importance of plasma protein binding in drug discovery. *Expert Opinion on Drug Discovery* **2007**, *2*, 51. [CrossRef]

[10] Fanalia, G.; Masibc, A.; Trezza, V.; Marino, M.; Fasano, M.; Ascenzi, P. Human serum albumin: From bench to bedside. *Molecular Aspects of Medicine* **2012**, *33*, 209. [CrossRef]

[11] Buttar, D.; Colclough, N.; Gerhardt, S.; MacFaul, P. A.; Phillips, S. D.; Plowright, A.; Whittamore, P.; Tam, K.; Maskos, K.; Steinbacher, S.; Steuber, H. A combined spectroscopic and crystallographic approach to probing drug–human serum albumin interactions. *Bioorganic and Medicinal Chemistry* **2010**, *18*, 7486. [CrossRef]

[12] Xie, M. X.; Xu, X. Y.; Wang, Y. D. Interaction between hesperetin and human serum albumin revealed by spectroscopic methods. *Biochimica et Biophysica Acta* **2005**, *1724*, 215. [CrossRef]

[13] He, W. Y.; Li, Y.; Xue, C. X.; Hu, Z. D.; Chen, X. G.; Sheng, F. L. Effect of Chinese medicine alpinetin on the structure of human serum albumin. *Bioorganic and Medicinal Chemistry* **2005**, *13*, 1837. [CrossRef]

[14] Zhang, Y.; Li, Y.; Dong, L.; Li, J. Z.; He, W. Y.; Chen, X. G.; Hu, Z. D. Investigation of the interaction between naringin and human serum albumin. *Journal of Molecular Structure* **2008**, *875*, 1. [CrossRef]

[15] Chaves, O. A.; Cesarin-Sobrinho, D.; Sant'Anna, C. M. R.; de Carvalho, M. G.; Suzart, L. R.; Catunda-Junior, F. E. A.; Netto-Ferreira, J. C.; Ferreira, A. B. B. Probing the interaction between 7-O-β-D-glucopyranosyl-6-(3-methylbut-2-enyl)-5,40-dihydroxyflavonol with bovine serum albumin (BSA). *Journal of Photochemistry and Photobiology A: Chemistry* **2017**, *336*, 32. [CrossRef]

[16] Chaves, O. A.; Teixeira, F. S. M.; Guimarães, H. A.; Braz-Filho, R.; Vieira, I. J. C.; Sant'Anna, C. M. R.; Netto-Ferreira, J. C.; Cesarin-Sobrinho, D.; Ferreira, A. B. B. Studies of the Interaction between BSA and a plumeran indole alkaloid isolated from the stem bark of *Aspidosperma cylindrocarpon* (Apocynaceae).

Journal of the Brazilian Chemical Society **2017**, *28*, 1229. [CrossRef]

[17] Mandeville, J. S.; Froehlich, E.; Tajmir-Riahi, H. A. Study of curcumin and genistein interactions with human serum albumin. *Journal of Pharmaceutical and Biomedical Analysis* **2009**, *49*, 468. [CrossRef]

[18] Campos, V. A. C.; Júnior, H. M. S.; Oliveira, D. F.; de Carvalho, H. W. P.; Machado, A. R. T.; Tirelli, A. A. Antibacterial activity of propolis produced by Frieseomelittavaria. *Ciência e Agrotecnologia* **2011**, *35*, 1043. [CrossRef]

[19] Chaves, O. A.; Jesus, C. S. H.; Cruz, P. F.; Sant'Anna, C. M. R.; Brito, R. M. M.; Serpa, C. Evaluation by fluorescence, STD-NMR, docking and semi-empirical calculations of the *o*-NBA photo-acid interaction with BSA. *Spectrochimica Acta Part A: Molecular and Biomolecular Spectroscopy* **2016**, *169*, 175. [CrossRef]

[20] Chaves, O. A.; da Silva, V. A.; Sant'Anna, C. M. R.; Ferreira, A. B. B.; Ribeiro, T. A. N.; de Carvalho, M. G.; Cesarin-Sobrinho, D.; Netto-Ferreira, J. C. Binding studies of lophirone B with bovine serum albumin (BSA): Combination of spectroscopic and molecular docking techniques. *Journal of Molecular Structure* **2017**, *1128*, 606. [CrossRef]

[21] Jiang, H.; Chen, R.; Pu, H. Study on the interaction between tabersonine and human serum albumin by optical spectroscopy and molecular modeling methods. *Journal of Luminescence* **2012**, *132*, 592. [CrossRef]

[22] Chaves, O. A.; Mathew, B.; Cesarin-Sobrinho, D.; Lakshminarayanan, B.; Joy, M.; Mathew, G. E.; Suresh, J.; Netto-Ferreira, J. C. Spectroscopic, zeta potential and molecular docking analysis on the interaction between human serum albumin and halogenated thienyl chalcones. *Journal of Molecular Liquids* **2017**, *242*, 1018. [CrossRef]

[23] Wardell, M.; Wang, Z.; Ho, J. X.; Robert, J.; Ruker, F.; Ruble, J.; Carter, D. C. The atomic structure of human methemalbumin at 1.9 A. *Biochemical and Biophysical Research Communications* **2002**, *291,* 913. [CrossRef]

[24] Hu, Y.-J.; Yue, H.-L.; Li, X.-L.; Zhang, S.-S.; Tang, E.; Zhang, L.-P. Molecular spectroscopic studies on the interaction of morin with bovine serum albumin. *Journal of Photochemistry and Photobiology B: Biology* **2012**, *112*, 16. [CrossRef]

[25] Stephens, P. J.; Devlin, F. J.; Chabalowski, C. F.; Frisch, M. J. Ab initio calculation of vibrational absorption and circular dichroism spectra using density functional force fields. *The Journal of Physical Chemistry* **1994**, *98*, 11623. [CrossRef]

[26] Tirado-Rives, J.; Jorgensen, W. L. Performance of B3LYP density functional methods for a large set of organic molecules. *Journal of Chemical Theory and Computation* **2008**, *4*, 297. [CrossRef]

[27] Hehre, W. J., A Guide to Molecular Mechanics and Quantum Chemical Calculations. Disponível em: <https://www.wavefun.com/?s=Files/AGuidetoMM.pdf>. Acesso em: 25 novembro 2018.

[28] The Cambridge Crystallographic Data Centre (CCDC). Disponível em: <http://www.ccdc.cam.ac.uk/solutions/csd-discovery/components/gold/>. Acesso em: 25 novembro 2018.

[29] DeLano, W. L.; PyMOL User's Guide; DeLano Scientific LLC. Disponível em: <http://pymol.sourceforge.net/newman/userman.pdf>. Acesso em: 25 novembro 2018.

[30] Chaves, O. A.; Amorim, A. P. O.; Castro, L. H. E.; Sant'Anna, C. M. R.; de Oliveira, M. C. C.; Cesarin-Sobrinho, D.; Netto-Ferreira, J. C.; Ferreira, A. B. B. Fluorescence and docking studies of the interaction between human serum albumin and pheophytin. *Molecules* **2015**, *20,* 19526. [CrossRef]

[31] Chaves, O. A.; de Oliveira, C. H. C. S.; Ferreira, R. C.; Pereira, R. P.; de Melos, J. L. R.; Rodrigues-Santos, C. E.; Echevarria, A.; Cesarin-Sobrinho, D. Investigation of interaction between human plasmatic albumin and potential fluorinated anti-trypanosomal drugs. *Journal of Fluorine Chemistry* **2017**, *199*, 103. [CrossRef]

[32] Manjushree, M.; Revanasiddappa, H. D. Interpretation of the binding interaction between bupropion hydrochloride with human serum albumin: A collective spectroscopic and computational approach. *Spectrochimica Acta Part A: Molecular and Biomolecular Spectroscopy* **2019**, *209*, 264. [CrossRef]

[33] Lakowicz, J. R.; *Principles of Fluorescence Spectroscopy*, 3rd. ed., Springer: New York, 2006.
[34] Ferreira, R. C.; Chaves, O. A.; de Oliveira, C. H. C. S.; Ferreira, S. B.; Ferreira, V. F.; Sant'Anna, C. M. R.; Cesarin-Sobrinho, D.; Netto-Ferreira, J. C. Drug-protein interaction: spectroscopic and theoretical analysis on the association between HSA and 1,4-naphthoquinone derivatives. *Revista Virtual de Química* **2018**, *10*, 432. [CrossRef]
[35] Gan, N.; Sun, Q.; Tang, P.; Wu, D.; Xie, T.; Zhang, Y.; Li, H. Determination of interactions between human serum albumin and niraparib through multi-spectroscopic and computational methods. *Spectrochimica Acta Part A: Molecular and Biomolecular Spectroscopy* **2019**, *206*, 126. [CrossRef].
[36] Wang, Q.; Ma, X.; He, J.; Li, Y.; Li, H. Insights into the fatty acid ester norethisterone enanthate binding to human albumin: fluorescence, circular dichroism, and docking investigations. *RSC Adv* **2015**, *5*, 44696. [CrossRef].
[37] Arık, M.; Çelebi, N.; Onganer, Y. Fluorescence quenching of fluorescein with molecular oxygen in solution. *Journal of Photochemistry and Photobiology A: Chemistry* **2005**, *170*, 105. [CrossRef]
[38] Montalti, M.; Credi, A.; Prodi, L.; Gandolfi, M.T; *Handbook of Photochemistry*, 3rd ed., Taylor & Francis: UK, 2006.
[39] Sun, H.; Liu, Y.; Li, M.; Han, S.; Yang, X.; Liu, R. Toxic effects of chrysoidine on human serum albumin: isothermal titration calorimetry and spectroscopic investigations. *Luminescence* **2016**, *31*, 335. [CrossRef]
[40] Chaves, O. A.; Jesus, C. S. H.; Henriques, E. S.; Brito, R. M. M.; Serpa, C. *In situ* ultra-fast heat deposition does not perturb the structure of serum albumin. *Photochemistry & Photobiology Science* **2016**, *15*, 1524. [CrossRef]
[41] Zhang, D.; Zhang, X.; Liu, Y. -C.; Huang, S. -C.; Ouyang, Y.; Hu, Y. -J. Investigations of the molecular interactions between nisoldipine and human serum albumin in vitro using multi-spectroscopy, electrochemistry and docking studies. *Journal of Molecular Liquids* **2018**, *258*, 155. [CrossRef]
[42] Zhang, Z.; Tang, R. Synthesis and fluorescence properties of Tb(III) complex with a novel β-diketone ligand as well as spectroscopic studies on the interaction between Tb(III) complex and bovine serum albumin. *Journal of Molecular Structure* **2012**, *1010*, 116. [CrossRef]
[43] Chatterjee, T.; Pal, A.; Dey, S.; Chatterjee, B. K.; Chakrabarti, P. Interaction of virstatin with human serum albumin: spectroscopic analysis and molecular modeling. *PLoS One* **2012**, *7*, e37468. [CrossRef]
[44] Berova, N.; Nakanishi, K.; Woody, R.W; *Circular dichroism: Principles and applications*, 2nd ed., Wiley: New York, 2000.
[45] Matei, I.; Hillebrand, M. Interaction of kaempferol with human serum albumin: A fluorescence and circular dichroism study. *Journal of Pharmaceutical and Biomedical Analysis* **2010**, *51*, 768. [CrossRef]
[46] Hosainzadeh, A.; Gharanfoli, M.; Saberi, M. R.; Chamani, J. K. Probing the interaction of human serum albumin with bilirubin in the presence of aspirin by multi-spectroscopic, molecular modeling and zeta potential techniques: Insight on binary and ternary systems. *Journal of Biomolecular Structure and Dynamics* **2012**, *29*, 1013. [CrossRef]
[47] Chaves, O. A.; Tavares, M. T.; Cunha, M. R.; Parise-Filho, R.; Sant'Anna, C. M. R.; Netto-Ferreira, J. C. Multi-spectroscopic and theoretical analysis on the interaction between human serum albumin and a capsaicin derivative-RPF101. *Biomolecules* **2018**, *8*, 78. [CrossRef]
[48] Temboot, P.; Usman, F.; Ul-Haq, Z.; Khalil, R.; Srichana, T. Biomolecular interactions of amphotericin B nanomicelles with serum albumins: A combined biophysical and molecular docking approach. *Spectrochimica Acta Part A: Molecular and Biomolecular Spectroscopy* **2018**, *205*, 442. [CrossRef]
[49] Camuri, I. J.; Costa, A. B.; Ito, A. S.; Pazin, W. M. Optical absorption and fluorescence spectroscopy studies of Artepillin C, the major component of green propolis. *Spectrochimica Acta Part A: Molecular and Biomolecular Spectroscopy* **2018**, *198*, 71. [CrossRef]